

Influence of Sea-States Description on Wave Energy Production Assessment

M-A. Kerbiriou, M. Prevosto, C. Maisondieu¹, A. Clément, A. Babarit²

¹ IFREMER, ERT/Hydrodynamics - Metocean Department,
BP 70 - 29280 PLOUZANE

²Ecole Centrale de Nantes, LFM,
BP 92101 - 44321 NANTES

Abstract

Sea-states are usually described by a single set of 5 parameters, no matter the actual number of wave systems they contain. We present an original numerical method to extract from directional spectra the significant systems constituting of a complex sea-state. An accurate description of the energy distribution is then given by multiple sets of parameters. We use these results to assess the wave climatology in the Bay of Biscay and to estimate the power harnessable in this area by a particular Wave Energy Converter, the *SEAREV*. Results show that the fine description of sea-states yields a better assessment of the instantaneous device response. The discrepancy between the classical and multi-sets descriptions shows that the new one is preferable for the assessment of harnessable power and for device design.

Keywords: Sea-States, Spectral Data, Systems Extraction, Wave Energy.

INTRODUCTION

Sea-states climatology is required for various applications, such as naval engineering, coastal management, design of fixed or floating structures, or natural hazard assessment. The common description of sea-states generally considers the existence of one single consistent wave system, in order to reduce the number of representing parameters. However this method, whereas it makes the data management easier and provides sufficient elements for most of analysis and applications, does not reflect the complexity of the really encountered sea-states. The availability of accurate directional measurements from SAR or buoys networks or from wave models shows that most of sea-states are made of two or more superimposed wave systems, of which characteristics evolve in time,

and of which energetic and dynamic contributions compared to each other are not easy to model by simple, fixed assumptions.

In the present study, we address the influence of the choice of sea-states description on wave energy harnessing. Two methods of assessment of available power are presented. The first, with the classical, single set of parameters $[f_p, H_s, \gamma, \theta, \sigma]$, where f_p is the frequency of the maximum spectral energy density, H_s the total significant wave height, γ the shape parameter of the frequency distribution, θ the mean direction at peak frequency and σ the directional spreading. The second is based on the spectrum partitioning, which yields a number n of coexisting significant wave systems, each described with the same set of parameters assigned with a subscript i , $i = [1..n]$.

The influence of the chosen description on the performances of the *SEAREV* device ([5], [2]) is then addressed. Both methods of energy assessment show that the sea-states description is critical, and put forward the benefit of a detailed representation of wave energy content.

1 PARTITIONING METHOD

The fine description of sea-states lies on the accurate analysis of available spectral data. Two-dimensional spectral data $S(f, \theta, t)$ provided by ARGOS for the Bay of Biscay zone were used for the study. Data are outputs from WWII model, run on a $1^\circ \times 1.25^\circ$ grid covering North Atlantic. Spectral data have a 15° directional and a minimal 2.10^{-3} Hz frequency resolution, and simulation time step is 1 hour. The aim of the analysis is to provide an automated and synthetic representation of every instantaneous sea-state using a set of parameters as small as possible. The process to obtain this output is splitted into five stages here listed:

- The peaks isolation

- The peaks grouping
- The type classification
- The analytic fitting
- The dynamical tracking

The fourth step (dynamical tracking) is optional, but helps for the classification and provides enlightenments on the local climatology. The analysis program is developed in the Matlab environment.

1.1 Peaks Isolation

This first step consists in extracting the distinct components of the sea-state from its 2D spectral representation. One of the first extraction processes was made by Gerling [6], 1992, with a technique of one-dimensional spectra thresholding. This method was modified by, among others, Hasselman & al, [9] 1996, or Hanson & Phillips [8] 2001, who treated the 2D spectrum $S(f, \theta)$ like a reversed topography including catchment areas. The peaks in the directional spectrum are then found by following the paths of strongest gradient leading to a same point. The Matlab routine *watershed* designed for hydrological purposes can be used to identify easily the "catchment areas" in the upside-down spectrum, corresponding to the spectral peaks.

The first thing is to make all the spectral distribution connected in the 2D plan; systems coming from North (absolute direction 0 or 360 °) are actually split over both sides of the θ axis. First we find the direction which minimizes the sum of spectral density along frequency. The whole 2D spectrum is then shifted in direction so that the ends of the new θ axis contain the minimum of energy.

Depending on the spectral data roughness, resolution or accuracy of extraction required by the user, the results of isolation process can be appreciably modified by the change of the connectivity parameter of the Watershed function, which induces a sensitivity change in the search of the maximum gradient path. In the strictest configuration and for complex sea-states data, the number of extracted components can reach 9.

1.2 Peaks grouping

Because of the sensitivity of the extraction method, all the isolated spectral components are not consistent wave systems and can be regarded as noise. Next stage of analysis consists in gathering meaningless components into physically valid wave systems. Two methods were used by several authors; the first one ([11], [1]) consists in computing a squared distance between two peaks a and b , $D_p(a, b)$, in the (f, θ) plan (1), and a spectral spreading $d_p(i)$, $i = a, b$ for each component, as follows (2):

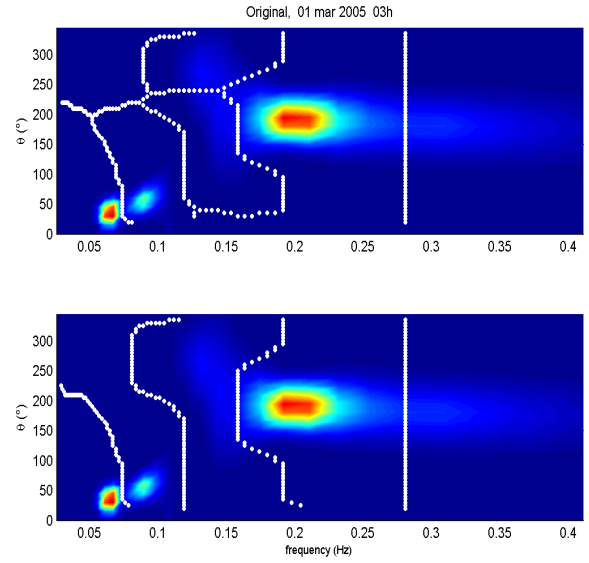


Figure 1: Wave Spectrum partitioning before (top) and after grouping (bottom).

$$D_p(i, j) = (fx(i) - fx(j))^2 + (fy(i) - fy(j))^2 \quad (1)$$

$$d_p(i) = \langle (fx(i) - \bar{fx})^2 \rangle + \langle (fy(i) - \bar{fy})^2 \rangle, \quad i = a, b \quad (2)$$

$$fx = f \cos \theta$$

$$fy = f \sin \theta$$

The two systems a and b are then merged if

$$D_p(a, b) < \kappa \max(d_p(a), d_p(b)) \quad (3)$$

with κ user-defined.

Some authors also compare the height of the saddle point to the height of the lowest peak in the omnidirectional spectrum.

The other method states that two spectral components a and b are merged if they satisfy two separate conditions about the gaps between the peak frequencies and the peak frequency directions as follows (4):

$$[|\theta_p(a) - \theta_p(b)| \leq \kappa_\theta] \cap [|f_p(a) - f_p(b)| \leq \kappa_f] \quad (4)$$

This method has been chosen because it is more flexible than the first one, and helps keeping apart systems of close instantaneous characteristics but different in origin and history. On the one hand, the overlapping of two components in the spectral domain does not imply that they are parts of a single wave system. This overlapping is taken into account in the next steps of the analysis, by computing the cross-influence of the components (1.3.2). On the other hand, as two or more swell systems can exist at the same time and as a swell system evolves in significant wave height independantly of the others, the criterion about the height of the saddle point has not been used for the grouping process.

The thresholds κ_θ and κ_f are user-tunable, depending on the local wave dynamics. They also depend on the data grid resolution. It seems reasonable that two neighbouring peaks are grouped if their frequency gap is smaller than 2 frequency increments, so κ_f was set to $2 \Delta f(f)$. Due to the somewhat higher uncertainty of direction measurements, the grouping threshold κ_θ was set to $\frac{\pi}{4}$.

Fig. 1 shows the spectrum partitioning for a date of Bay of Biscay data, before and after grouping stage. Limit between peaks is materialized by white border lines.

Every extracted subset of the spectrum can then be considered as an isolated wave system. Indeed, one computes all its moments and derived quantities among which: the significant wave height $H_s = 4,004\sqrt{m_0}$, the mean frequency $f_m = \frac{m_0}{m_1}$, the bandwidth parameter $\nu = \sqrt{\frac{m_0 m_2}{m_1^2 - 1}}$, the directionnal spreading $\sigma = \sqrt{(\iint (\theta - \theta_m)^2 S(f, \theta) \Delta f \Delta \theta / m_0)}$. The peak frequency at this stage can only take discrete values and its estimation needs the analytical fitting processed in a next step.

1.2.1 Primary classification

For more accurate subsequent computations, one needs to know the type of each wave system, namely swell or wind sea. When the wind data are available (strength U_w and direction θ_w), wind sea and swell systems are split according to the separation frequency f_s (5), like in Aarnes & Krogstad [1], or Hwang & Wang [12]:

$$f_s = \frac{g}{\beta 2\pi U_w |\cos(\theta_w - \theta_m)|} \quad (5)$$

with $\theta_m = \text{mean system direction}$, $\beta = 4/3$

A system is classified in wind-sea type if $f_p > f_s$ and $|\cos(\theta_w - \theta_m)| \leq \frac{\pi}{2}$, in swell type in other cases. f_p is known within one grid increment at this stage, and this classification is temporary.

If wind data is not available, a default separation frequency is set, to be tuned to the local dynamics of winds and waves.

Due to the different time variabilities of wind and waves, this criterion is not always successful. This classification is needed to choose the treatment further applied to each system, but an additional stage consists in using the dynamical tracking (which will not be presented here) to definitely identify the type of the time-followed systems, hence of every instantaneous wave system. A time-coherent system is then assigned the same type all along its persistence, which avoids resorting to ‘hybrid’ or ‘Old Wind Sea’ types.

1.3 Analytic fitting

The aim of this stage is to give a description of every system constituting of a sea-state with a homogeneous set of variables. Two well-known analytical functions are chosen to fit the frequential and directional distributions of each individual spectrum. The final parameterized function which best fits the original system spectrum $S(f, \theta)$ is the product $\tilde{S}(f, \theta) = \tilde{S}_f(f) \tilde{S}_\theta(\theta)$.

The directional distribution is modelled by the classical \cos^{2s} function, where s is computed iteratively to minimize the square error between the original frequency-integrated directional distribution $S_\theta(\theta) = \int S(f, \theta) df$ and the analytic directional distribution.

1.3.1 Modified JONSWAP function

The frequential distribution of the omni-directional spectrum ($S_f(f) = \int_0^{2\pi} S(f, \theta) d\theta$) is modelled by a modified JONSWAP function of which the governing parameters are f_p , H_s and γ . As the JONSWAP function was designed to accurately model wind seas, it does not adapt quite as good to swell systems which usually show steeper shapes. Consequently, the variation rate of the function is modified by changing the exponent in the JONSWAP function now written as (6):

$$\begin{aligned} \tilde{S}_f(f) &= \alpha \frac{g^2}{(2\pi)^4} \left(\frac{f}{f_p}\right)^{-5+p} e^{-\frac{5}{4}\left(\frac{f}{f_p}\right)^{-4+p}} \gamma^a \quad (6) \\ a &= e^{\frac{(f-f_p)^2}{2\sigma^2}} \\ \sigma &= 0.07, \\ \sigma &= 0.09, \\ \alpha | H_s^2 &= 16 \int_0^\infty \tilde{S}_f(f) df \end{aligned}$$

If the wave system is of wind sea type, a classical JONSWAP function is used, defined by the set of variables $[f_p, H_s, \gamma]$. For swell systems, p is set to -2, giving steeper slopes than the ones of a classical JONSWAP formulation. In all cases, the set $[f_p, H_s, \gamma]$ is computed by an iterative linear solver which fits the best function to the original omni-directional spectrum $S_f(f)$ in the least square sense. This procedure finds the best compromise values between the three parameters, starting from the values of H_s and f_p computed previously, and $\gamma = 1$. As f_p is free to vary, it now can take continuous values where $\tilde{S}_f(f)$ is defined, whereas it previously had discrete value depending on the original spectrum resolution.

1.3.2 Cross-influence correction

As was mentioned above, the systems extracted from the original spectrum may partially overlap each other, due to their frequential and directional spreadings. The

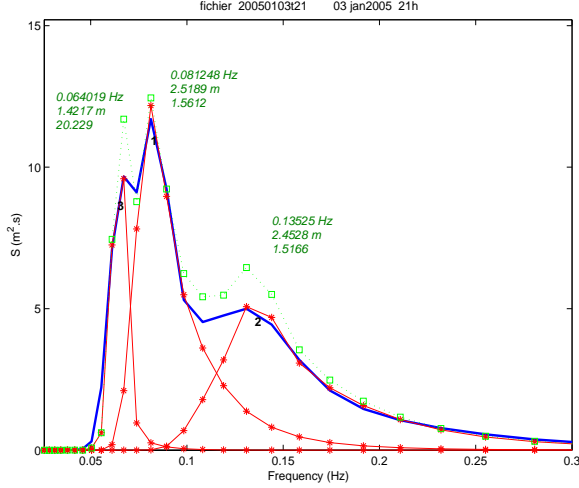


Figure 2: Analytic fitting before overlapping correction; blue=original 1D spectrum, red=individual components, green=sum of components.

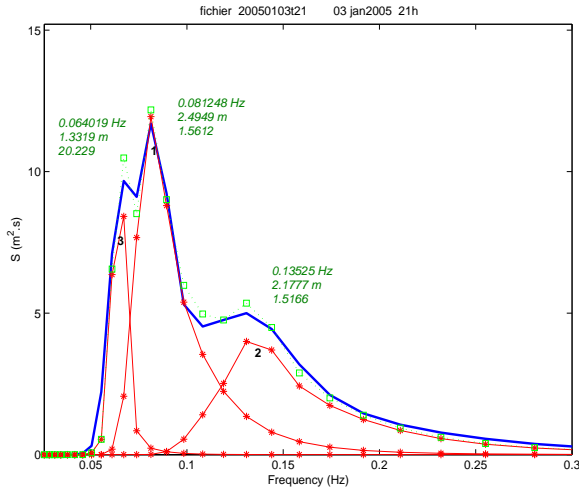


Figure 3: Analytic fitting after overlapping correction. Same legend as Fig. 2.

next step of the process consists in computing the overlapping in order to correct the respective H_s of each system. This correction has no effect on the value of f_p , and we neglect the modification it may induce on the values of γ .

The correction is performed in frequency domain, when omni-directional individual spectra have been fitted a modified JONSWAP function, so that every system i is modelled by:

$$S_i = \tilde{S}(H_{s_i}, f_{p_i}, \gamma_i) \quad (7)$$

The cross-influence of each modelled system to each other is computed in a matrix C where elements C_{ij} are :

$$C_{ij} = S_i(f_{p_j}) \quad (8)$$

and the correction coefficients c of each system is computed such as:

$$C \times c = [S_i(f_{p_i})] \quad (9)$$

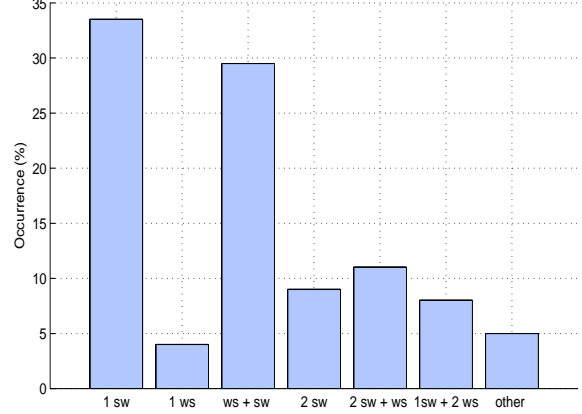


Figure 4: Number and type of simultaneous systems. 'WS' = Wind Sea; 'SW' = Swell; 'Other': 3 swells or more than 3 systems.

The corrected H'_{s_i} is now

$$H'_{s_i} = \sqrt{c_i} H_{s_i} \quad (10)$$

The interest of this correction is illustrated on Fig. 2 and Fig. 3

2 Bay of Biscay Available Power

Wave climate in the Bay of Biscay is assessed through the analysis of one year of data (January-December 2005). This set of data is obviously not long enough to perform a statistical study of seasonal variations and describe an accurate climatology, but it is sufficient to point out a wide variety of complex configurations with significant occurrences.

The number of distinct wave systems within a sea-state is the first variable we observe. From systems partitioning and classification, counting wave configurations all over year 2005 yields the result shown on Fig. 4.

One-system configurations (one swell or one wind sea) count for only about 37% of the observed cases. This means that the classical simplified sea-state description is erroneous 63% of time. Configurations with 2 systems are most often made of one swell and one wind sea (30%), and the superimposition of two swells occurs nearly 9% of the time. 3-systems configurations appear 18% of the time, with 2 swells + 1 wind sea, and with a surprisingly high occurrence of 1 swell + 2 wind seas, which is mainly an effect of the time data averaging duration. The 'other' category contains all the cases of 3 swells (seldom) or more than 3 systems.

A complete review of the wave climatology elements established from the Bay of Biscay data analysis will be

presented in a subsequent paper; major results regarding wave energy harnessing can however be summarized in the points hereafter:

- More than 17000 separate systems were identified over 8760 hours of spectral data, which yields an average number of 2 simultaneous systems per sea-state. Number of simultaneous systems varies between 1 and 5, with a small proportion of sea-states with more than 3 systems (Fig. 4). Among these systems, 10900 are of swell type and 6100 are of wind sea type.
- Most of the incoming energy (80%) enters in the sector WSW-NW, about 60° wide. Swell systems directions are restricted to this sector; wind sea directions cover the 360°, with a homogeneous repartition.
- Most of incoming power and considerable amount of year-cumulated significant wave height are due to swell in the frequency range [0.05 – 0.11Hz].

2.1 Annual power estimate

The power per unit crest length developed by a sea-state is usually defined as in Tucker, 1991 [10]:

$$P_{00} = \frac{\rho g^2}{4\pi} m_{-1} \quad (11)$$

$$m_{-1} = \int \frac{S_u(f)}{f} df \quad (12)$$

When using partitioned sea-states, we assume that the total developed power is the sum of the power of each identified wave system, such as:

$$P_0 = \sum_{i=1:n} P_{0i}$$

$$P_{0i} = \frac{\rho g^2}{4\pi} \int \frac{S_{u_i}(f)}{f} df \quad (13)$$

In any case, the power varies with the squared SWH and the inverse energy frequency ($f_e = m_0/m_{-1}$), the latter being affected by the bandwidth of the spectrum. For single systems, swells carry more power than wind seas of same significant wave height.

Two computations of the power were made for comparison at each date all along the year 2005: with the single set of parameters (P_{00} using the parameters SWH_0 , f_{p0} , θ_{p0} , σ_0 and γ_0) and with the n sets of parameters for the n identified wave systems (P_{0i} using SWH_i , f_{pi} , θ_{pi} , σ_i and γ_i , $i=[1:n]$). Figure 5 shows the computed power (top plot) and the instantaneous difference between the two computations (bottom plot). The difference is near zero when sea-states are made of one single system; greatest values are reached (up to 100%) for sea-states made of several systems. In these cases difference can be either negative or positive, depending on the frequency

distribution of the energy: if most of the spectral energy density lies at high frequencies (sea-state dominated by wind sea) but a part is contained in swell system, the energy frequency f_e of the total spectrum would be shifted to a lower value and the associated total power overestimated. Conversely if the sea-state is dominated by swell but contains wind-sea component, the computed total power would be underestimated.

The difference averaged over the whole year shows that the classical computation of power results in a 10% underestimate of the annual mean available power. The method based on partitioning yields an average annual power of about 23 kW.m^{-1} whereas a value of 21 kW.m^{-1} is given by the classical method. This bias itself is acceptable, but masks a strong discrepancy of the instantaneous estimates. When the accurate knowledge of energy distribution is required, as for wave energy harnessing by resonant devices, the single-set method may lead to erroneous conclusions.

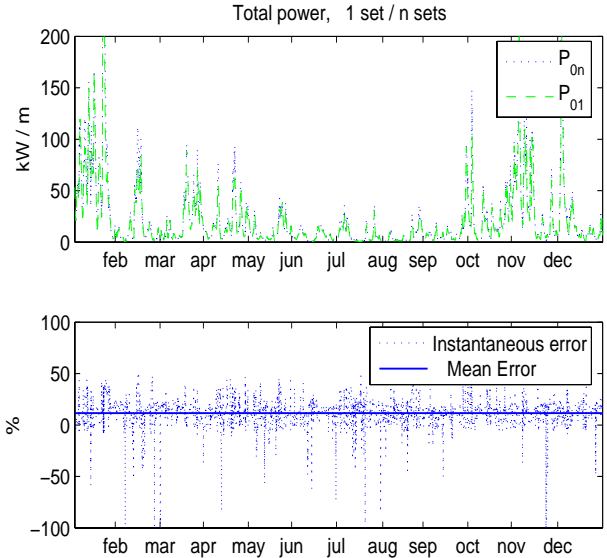


Figure 5: Instantaneous developed power along year 2005.

3 SEAREV DEVICE

The SEAREV is a floating, completely enclosed device, with an internal moving mass. Under the action of waves, the floating hull and the internal moving mass will move, each having its own dynamics. The relative motion between the floating body and the moving mass is used to drive a generator via an hydraulic device, the Power Take Off (PTO).

This device offers many advantages :

- All the moving parts are located inside the hull of the floating body, so they are protected from the action of sea water. Thus, the maintenance costs and the risk of failure are expected to be lower than for a system whose moving parts are in contact with sea water.

- The internal mass is a large heavy cylinder featuring an off-centered gravity center, Fig. 6, which is the main difference to the PS frog device [4]. This means that the mechanism needs no end stops. The inner cylinder is able to make several full revolutions around its horizontal axis, or, from another point of view, the floating body can do a full revolution around the cylinder without destruction. So the device is expected to have a high survivability in extreme waves.
- The device does not need any external reference. It is a self-referenced WEC, which means that each part of the device, the hull and the cylinder, is a reference for the other. As it doesn't use the seabed as a reference, it needs only slack moorings, which are naturally less expensive than tight ones.

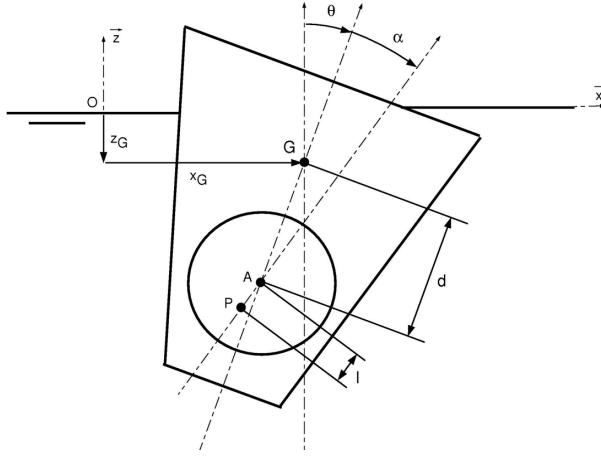


Figure 6: Notations

A more detailed description of the SEAREV mechanical characteristics can be found in [5] or in [2]. The modelling computations of wave energy extraction are performed in the linear theory approach. The device is equipped with a dynamical latching control of the internal moving mass, in order to make the best of a wide range of wave systems with various peak frequency and bandwidth.

Sensitivity tests were made to assess the influence of the wave systems describing parameters, briefly summarized below:

- Due to the pendular motion SEAREV is direction-sensitive. However, thanks to its geometry, very good production results maintain for wave systems incoming in the range 0° - 45° (relatively to the bow of the device). The efficient open sector is then 90° wide, which allows the device to take advantage of most of the sea-state configurations.
- The directional spreading increasing in the range $[0 - 50^\circ]$ is lightly favourable to the device operation, with a slight improvement of performance.
- The dependency of the production to the squared significant wave height is known to be linear (with latching control off).

4 SEAREV PERFORMANCES

4.1 Test-case study

The SEAREV numerical model was run with inputs from realistic sea-states picked up from the 2005 year data and representative of the Bay of Biscay climatology. The case presented here illustrates one of the most common configurations: 2 systems, 1 swell + 1 wind sea, coming from West and only 7° apart. The total significant wave height is 2.2 meters, respectively 1.8 m for swell and 1.25 m for wind sea. The SEAREV is West-oriented, both systems coming nearly as head sea.

This case is not particularly favourable to the SEAREV, because the peak frequencies of both systems are relatively far from the device natural frequency. The aim of the experiment is to show to which extent the choice of the sea-state description method can strongly affect the harnessable energy assessment.

The model was run with 4 different inputs :

- The two first time series are built from each of the two systems separately.
 - In the third run, the numerical model uses the superimposed two time series to compute a total excitation force and the resulting movements.
 - The fourth consists in constructing a time series from the unique global set of parameters.
- All the runs are performed with the latching control off, because the analysis of the results becomes more delicate when latching control is applied. The spectral inputs are plotted on Fig. 7. A significant simulation duration was obtained by performing fifteen 400-seconds runs, each with a different random phase draw. The output energy (averaged over the 15 runs) of this test-case simulation is shown Fig. 8. Output energy values are made dimensionless by the result of the configuration with the superimposed time series.

- The optimal work frequency f_{op} of the device is 0.125Hz (8s). A good functioning is found in the range 0.1-0.14 Hz, with a power ratio over 75%.
- Increasing the bandwidth (computed as $\nu = \sqrt{\frac{m_0 m_2}{m_1^2 - 1}}$) is found to have a positive influence on the device performance before the optimal frequency, becoming slightly negative at higher frequencies.

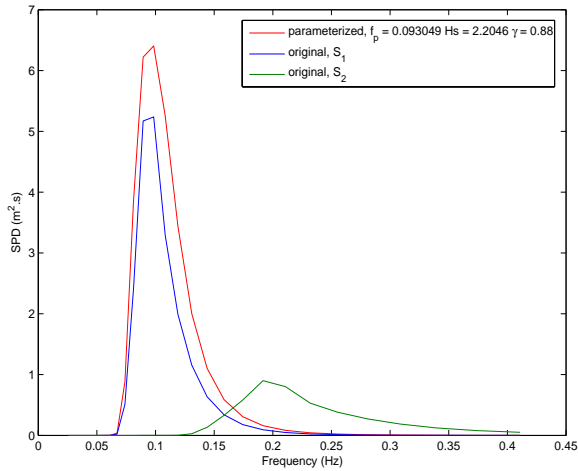


Figure 7: Separate and parameterized input systems. Swell system (blue), wind sea (green), parameterized (red).

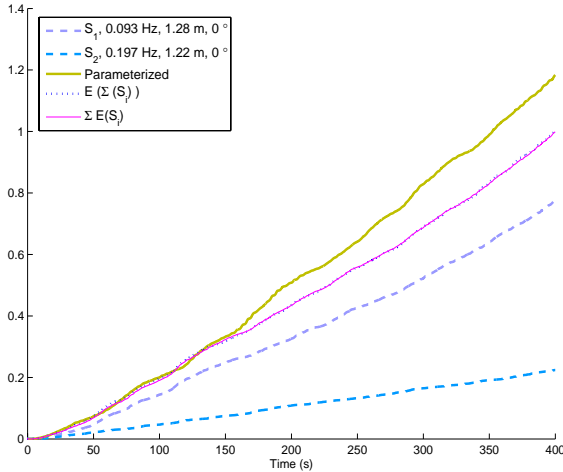


Figure 8: SEAREV response in two-systems sea-state.

Comparing the results from the individual systems (swell S_1 and wind sea S_2), the device works much better with the swell system of which the peak frequency is the closest to f_{op} . This swell ($f_p = 0.09\text{Hz}$) is not in the most interesting range for the SEAREV functioning, for which short swells in the range $[0.1-0.11\text{Hz}]$ are more appropriate, but is still much more efficient than the high frequency wind sea.

We note that in this case, the sum of the productions by the separate systems exactly equals the production of the sum of the systems ($\sum E(S_i) = E(\Sigma(S_i))$). This is normally the case when the total duration of the simulation is long enough, according to the linear assumptions underlying the excitation force computation.

Most important for the present study is the difference obtained using the parameterized description, for which the produced energy is 17% higher. This is due to the fact that the amount of spectral power density from wind

sea is attributed to the best working system (swell), not in agreement with the real physical distribution of energy in the sea-state (Fig. 7). Assuming that the linear hypothesis is valid, the real power production in this configuration should be closer to the one of the superimposed input, $E(\Sigma(S_i))$.

What happens in this case would happen everytime the sea-state is made of more than one wave system. In the classical parameterized description the dominating system in the spectral power density distribution artificially absorbs the energy of the other components, yielding an erroneous input to the device (underestimate or overestimate of the available power, see 2.1). The resulting harnessed power ratio may as well be underestimated or overestimated, depending on the adequacy of the modelled input spectrum to the frequency response of the device.

The observations we make here for this precise case have a qualitative significance, and show that the error about energy harnessing can be large; yet this example does not presume the sense of the error in other configurations.

4.2 SEAREV annual production assessment

The SEAREV power ratio function r based on the 5 describing parameters is built from the sensitivity tests, assuming that the parameters are independant (except for f_p and γ , which are clearly interdependant regarding the device response). Knowing at each date the characteristics of each wave system in the sea-state, r can be used to assess the harnessable power. The whole year sea-states description is passed through the power ratio function, first using the partitioned systems and the corresponding n sets of parameters, and second using the classical single set of parameters. For the first computation, following the linear hypothesis we assume that the total extracted power is the perfect sum of the power extracted from each individual system.

4.2.1 Adequacy to resource characteristics

SEAREV was designed to extract a maximum amount of energy with manageable dimensions. As its characteristic length is about 20 m and its natural period 8 s (0.125 Hz), it is especially fit to work with short wavelength swell systems or old developed wind seas, in frequency range $[0.1 - 0.14 \text{ Hz}]$. The adequacy of its frequency response to the SWH-frequency distribution in the Bay of Biscay is qualitatively pointed out on Fig. 9.

The exploitable wave systems represent about 30% of the incoming SWH. About 40% of the incoming SWH is contained in low frequency swell systems below 0.1 Hz, but harnessing efficiently this wave power would require device dimensions inconceivable at the moment.

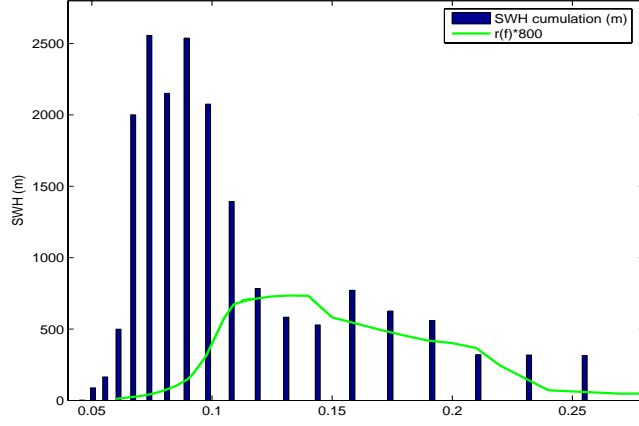


Figure 9: Cumulative SWH per frequency band for year 2005, and expanded frequency response of the SEAREV

4.2.2 Experiment

As no information is known yet about the actual dynamical behaviour of the SEAREV in real sea-states, and particularly the orientation it would take under influence of mooring, wind and waves of different wavelengths and heights, the computation was realised in making the SEAREV device turn inside a 180° sector, from southward-oriented (absolute direction $\theta = 180^\circ$) to northward-oriented (absolute direction $\theta = 0^\circ$) per 10° steps. For each direction of the device and each date, the harnessed power is computed. P_{hp} and $\overline{r_{hp}}$ are respectively the harnessed power [14] and the year-averaged power ratio using partitioned description [16], P_{hs} and $\overline{r_{hs}}$ are the harnessed power [15] and year-averaged power ratio using the single-set description [17]:

$$P_{hp}(t, \theta) = \sum_{i=1:n(t)} (r(f_{pi}, (\theta_{pi} - \theta), \sigma_i, \gamma_i) \times P_{0i}(t)) \quad (14)$$

$$P_{hs}(t, \theta) = r(f_{p0}, (\theta_{p0} - \theta), \sigma_0, \gamma_0) \times P_{00}(t) \quad (15)$$

$$\overline{r_{hp}}(\theta) = \frac{1}{T} \sum_{t=1:T} \frac{P_{hp}(t, \theta)}{P_0(t)} \quad (16)$$

$$\overline{r_{hs}}(\theta) = \frac{1}{T} \sum_{t=1:T} \frac{P_{hs}(t, \theta)}{P_{00}(t)} \quad (17)$$

$\overline{P_{hp}}(\theta)$ and $\overline{P_{hs}}(\theta)$ are the year-averaged harnessed powers from classical and partitioned descriptions respectively.

4.2.3 Results

Comparison of the results from the two methods are shown on Fig. 10. First curve ($\overline{P_{hp}}(\theta)/\overline{P_{hs}}(\theta)$) shows that the classical method tends to underestimate the harnessed power in a proportion of more than 15%, whatever

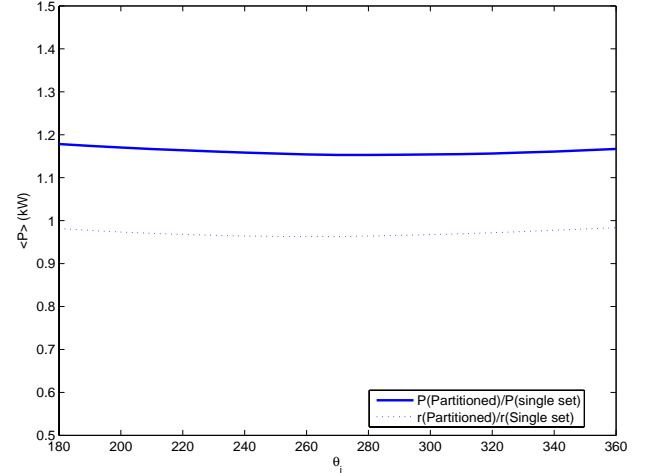


Figure 10: Ratio of power productions (solid line) and power ratios (dashed), from one-set and multi-set computations.

the direction of the device. In the case of the Bay of Biscay, as was stated from the elements of climatology, power density spectra are most often dominated by swell systems of low, or very low frequency. As the single set of parameters artificially modifies the energy distribution in frequency domain, the energy input is virtually shifted to the low frequencies. Consequently the spectrum taken as input does not match the frequency response of the device, whereas the real spectrum would do better; the energy content which may be present in the efficient medium frequency range [0.1-0.15 Hz] is not taken in account and the delivered power in the case of the single set description is therefore undervalued. In the cases when the spectral energy peak is found in the medium range (when sea-state is dominated by a developed wind sea or short North-West swell), the single-set description has an opposite effect in overestimating the power output. However, the occurrence of these situations does not counterbalance the more frequent underestimation.

In the opposite, the power ratio is slightly overestimated by the single-set method, around 3%. By computing the available power from the moments of the spectrum described by the single set of parameters, or by the sum of the powers contained in the individual wave systems, we saw that the single-set definition would lead to an underestimation of the available power. This results in an increased assessment of the single-set power ratio, and explains why the difference between $\overline{r_{hs}}$ and $\overline{r_{hp}}$ is small.

Let's note that these features about compared power outputs and power ratios are admissible only for the area studied in the Bay of Biscay and for the SEAREV device. Depending on the local wave climatology (several systems occurrence, strong predominance of swell or wind sea, systems directionality), and depending on the WEC properties (resonant or not, direction-dependent or other

characteristics), the effect of the single-set definition could be amplified or reduced relatively to the one we noticed in our case of interest.

5 CONCLUSIONS

A set of numerical tools was designed to perform accurate analysis of spectral wave data. For a given sea-state depicted by a frequency-direction 2D spectrum, more information is extracted regarding the global energy content, the number and type of wave systems, the frequential and directional distributions of each of them, their time evolution and origins. The output data are used to build a comprehensive climatological database which is used to discuss the harnessable energy assessment with a specific Wave Energy Converter, the *SEAREV* device.

The problem of the influence of the sea-states description on the estimation of the harnessable energy for a given device had not been addressed yet. Our work leads to a few answers.

First, the description of sea-states with a single set of parameters can lead to very large errors in the computation of the available power. In the Bay of Biscay, very large instantaneous errors are partly compensated by integration along the year, but in some other places it might not be the case, depending on the dominant wave climatology.

Second, for evaluation of mechanical systems such as wave energy converters the quality of the output data is conditioned by the quality of the input signal. We found that the classical description leads to erroneous inputs to the device, yielding obviously erroneous estimates of the instantaneous harnessed energy. Thus the multi-set description of sea states is more reliable to estimate the instantaneous power output and power ratio and this would be the case in any combination of WEC and production site.

When computing the long term energy production, the cumulation of the instantaneous errors can lead to a strong mistaking in the estimation. In the Bay of Biscay, characterized by a predominance of long swell systems, the single-set description most of time changes the virtual input to the *SEAREV* in the sense of a reduced agreement with the frequency response of the device. The result is a reduced estimate of the power harnessable by this device at this location.

The results we obtained are only valid for the particular combination Bay of Biscay-*SEAREV*; in another place or with another WEC, results could have been quantitatively different, but the estimation process and the comparison between the single-set method and the

partitioned method would still be consistent.

Because of the heavy investments required for the development and implementation of wave energy converters, overestimating energy potential may cause financial hazards, and because of the rarity of the available implementation zones, underestimating it could cause unnecessary disqualification of potential sites.

The time variability of available wave power is a major issue for the design of the wave energy converters and their electromechanical capacities. The occurrence of extreme wave heights is also of critical importance when considering the survivability of devices. The refined multi-set description of complex sea-states is certainly beneficial to studies addressing these points.

Acknowledgements

ARGOSS company provided wave spectral data from WaveWatch III model covering North-West of Atlantic. ARGOSS, p.o.box 61,8325 ZH Vollenhove, the Netherlands. <http://www.argoss.nl>

ADEME (Agence de l'Environnement et de la Maîtrise de l'Énergie) participates in funding.

References

- [1] J.E. Aarnes, H.E. Krogstad: *Partitioning sequences for the dissection of directional Ocean Wave Spectra: a Review*. Part of ENVIWAVE Project, 2001.
- [2] A. Babarit, A.H. Clément: *Optimal Latching Control of a Wave Energy Device in Regular and Irregular Waves*, Applied Ocean Research Vol 28,2, pp.77-9, 2006.
- [3] A. Babarit: *Optimisation hydrodynamique et contrôle optimal d'un récupérateur de l'énergie des vagues*, PhD thesis, Ecole Centrale de Nantes, 2005. in French.
- [4] R.H. Bracewell: *Frog and PS Frog: A Study of Two Reactionless Ocean Wave Energy Converters*. PhD thesis, Lancaster University, 1990.
- [5] Brevet FR (n° enregistrement 04 10 927, le 15 Octobre 2004 à Paris) /Système Electrique Autonome de Récupération de l'Énergie des Vagues/ (co-inventeurs A.H. Clément, A. Babarit, G. Duclos)
- [6] T. W. Gerling: *Partitioning Sequences and Arrays of directional Ocean Wave Spectra into Component Wave Systems*. Journal of atmospheric and Oceanic Technology, vol 9, pp 444-458, 1991.

- [7] B. Gjevik, H.E. Krogstad, A. Lygre, O. Rygg: *Long Period Swell Events on the Norwegian Shelf*. J. Phys. Ocean., 1988, 18, 724-737 .
- [8] J.L. Hanson, O.M. Phillips: *Automated Analysis of Ocean Surface Directional Wave Spectra*. Journal of atmospheric and Oceanic Technology, vol 18, pp 277-293, 2001.
- [9] Hasselman, C. Bruning, K. Hasselman, P. Heimbach: *An Improved Algorithm for the Retrieval of Ocean Wave Spectra from Synthetic Aperture Radar Image Spectra*. J. Geophys. Res., 101(C7) : 16,615-16,629, 1996.
- [10] M.J. Tucker: *Waves in Ocean Engineering; Measurement, Analysis, Interpretation*. Ellis Horwood series in Marine Science, 1991, 431pp.
- [11] A.C. Voorrips, V.K. Makin, S. Hasselman: *Assimilation of Wave Spectra from pitch and roll buoys in a North Sea Wave Model*. J. Geophysical Research, 1997, 102(C3) , pp 5829-5849.
- [12] D.W. Wang, P.A. Hwang: *An Operational Method for Separating Wind Sea and Swell from Ocean Wave Spectra*. Journal of Atmospheric and Oceanic Technology. Vol. 18, No. 12, pp. 2052-2062, 2001.